Chiroptical properties from time-dependent density functional theory. I. Circular dichroism spectra of organic molecules

Jochen Autschbach[a] and Tom Ziegler[b]
Department of Chemistry, The University of Calgary, 2500 University Drive NW, Calgary, Alberta T2N 1N4, Canada

Stan J. A. van Gisbergen
Scientific Computing and Modeling and Theoretical Chemistry, FEW, Vrije Universiteit, De Boelelaan 1083, 1081 HV Amsterdam, The Netherlands

Evert Jan Baerends
Theoretical Chemistry, FEW, Vrije Universiteit, De Boelelaan 1083, 1081 HV Amsterdam, The Netherlands

(Received 23 July 2001; accepted 28 November 2001)

We report the implementation of the computation of rotatory strengths, based on time-dependent density functional theory, within the Amsterdam Density Functional program. The code is applied to the simulation of circular dichroism spectra of small and moderately sized organic molecules, such as oxiranes, aziridines, cyclohexanone derivatives, and helicenes. Results agree favorably with experimental data, and with theoretical results for molecules that have been previously investigated by other authors. The efficient algorithms allow for the simulation of CD spectra of rather large molecules at a reasonable accuracy based on first-principles theory. The choice of the Kohn–Sham potential is a critical issue. It is found that standard gradient corrected functionals often yield the correct shape of the spectrum, but the computed excitation energies are systematically underestimated for the samples being studied. The recently developed exchange-correlation potentials ''GRAC'' and ''SAOP'' often yield much better agreement here with experiments for the excitation energies. The rotatory strengths of individual transitions are usually improved by these potentials as well. © *2002 American Institute of Physics.* [DOI: 10.1063/1.1436466]

I. INTRODUCTION

Optical activity is undoubtedly one of the most important topics in chemistry and biochemistry due to the ubiquitous presence of chiral molecules in living organisms. The structural aspects of chirality and their relation to the electronic structure manifest themselves in various optical and spectroscopical effects, such as optical rotation (OR), optical rotatory dispersion (ORD), and circular dichroism (CD). Since these techniques specifically distinguish between the optical antipodes that otherwise have the same physical properties, they are frequently employed tools in experimental studies of chiral substances. For that reason, the first-principles theory of optical activity has been of considerable interest since the early days of quantum mechanics. It is an important aspect of quantum chemistry to provide the methodology and the program code to allow for the computation of the respective properties.[1–5]

Density functional theory (DFT) has emerged as the currently most applied method for molecular computations due to its balance between accuracy and efficiency even for rather large systems. DFT was originally formulated as a time-independent theory for the nondegenerate ground state of an atom or a molecule. However, it has now been extended to the time-dependent (TD-DFT) realm[6–8] which allows for the application of the machinery of time/frequency-dependent response theory. Subsequently, methodology and calculations of excitation energies, frequency-dependent polarizabilities and hyperpolarizabilities, van der Waals coefficients, Raman spectra, etc., have been reported in the literature. It was found that the TD-DFT treatment offers greatly enhanced accuracy as compared to some of the more frequently used *ab initio* methods (RPA, CIS) at comparable or less computational expense, in particular as far as low-lying excitations are concerned.[9] TD-DFT implementations regarding optical activity have been reported recently for the frequency-dependent optical rotation parameter[10,11] within the Gaussian code, and for optical rotations and CD spectra within TURBOMOLE[12,13] and a numerical code.[14] Prior code developments for polarizabilities and excitation energies have been carried out by van Gisbergen *et al.*[15,16] for the AMSTERDAM DENSITY FUNCTIONAL Program suite (ADF),[17–20] by Casida *et al.*[21] for the DFT code DEMON, and by Bauernschmitt and Ahlrichs for TURBOMOLE.[9] An alternative molecular DFT implementation was reported in Ref. 22. A formulation of TD-DFT response theory that is generally applicable to molecular problems, and which we will use below, has been presented by Casida.[23]

It is our purpose here to report the expression for the optical rotation parameter β within the TD-DFT formulation on which the ADF RESPONSE module is based, and from this to extract the rotatory strengths R needed to simulate CD

[a]Author to whom correspondence should be addressed. Electronic mail: jautschb@ucalgary.ca
[b]Electronic mail: ziegler@chem.ucalgary.ca

spectra. Their computation makes extensive use of the machinery already available in ADF to calculate excitation energies and oscillator strengths, and only minor modifications are necessary to access these quantities. The code is applied to the calculation of rotatory strengths of low-lying transitions, and to the simulation of CD spectra, of a number of small and moderately sized organic molecules. The results are compared to experimental data and to previously reported theoretical results. The agreement with alternative theoretical TD-DFT results for the benchmark molecule methyloxirane is excellent. Further, very good agreement with previously published TD-DFT results and experimental spectra for penta- and hexahelicene is achieved. Generally, the agreement with experiment for our samples is quite reasonable, even though some effects that influence the experimental data have been neglected in the computations. For the case of the $n \rightarrow \pi^*$ transition of methyl-substituted cyclohexanones, we find that sign and magnitude of the rotatory strengths are very sensitive to the molecular geometries, basis sets, and the DFT potential being employed. An important aspect of this work is therefore the first application of the recently developed Kohn–Sham potentials "SAOP" and "GRAC" [24,25] to the computation of chiroptical properties.

Section II is devoted to the formalism and the methodology. In Sec. III, we describe the details of the computations, while the results are presented and discussed in Sec. IV. A short summary is given in Sec. V.

II. METHODOLOGY

The quantum theory of optical activity has been extensively described in early overview articles such as Refs. 1, 2, and 4. The optical rotation parameter arises in this framework from perturbations of the electric ($\boldsymbol{\mu}$) or magnetic ($\mathbf{m}$) dipole moments by a time-dependent magnetic or electric field, respectively. For $u, v \in \{x,y,z\}$, the time-dependent perturbations contribute to the induced dipole moments according to

$$\mu_u' = \sum_v \alpha_{uv} E_v - \sum_v \frac{\beta_{uv}}{c} \frac{\partial B_v}{\partial t} + \cdots, \tag{1a}$$

$$m_u' = \sum_v \kappa_{uv} B_v + \sum_v \frac{\beta_{uv}}{c} \frac{\partial E_v}{\partial t} + \cdots. \tag{1b}$$

See also Ref. 26. Here, α_{uv} and κ_{uv} are components of the electric polarizability tensor and the magnetic susceptibility tensor, respectively, while β_{uv} is a component of the optical rotation tensor. Its rotational average $\overline{\beta} = (1/3)(\beta_{xx} + \beta_{yy} + \beta_{zz})$ is the optical rotation parameter usually determined in experiments. The quantities α, κ, β,... are frequency dependent. From a sum-over-states (SOS) treatment in the time domain,[27] it is found that

$$\overline{\beta} = \frac{2c}{3} \sum_\lambda \frac{\mathrm{Im}(\boldsymbol{\mu}_{0\lambda} \cdot \mathbf{m}_{\lambda 0})}{\omega_{0\lambda}^2 - \omega^2} = \frac{2c}{3} \sum_\lambda \frac{R_{0\lambda}}{\omega_{0\lambda}^2 - \omega^2}, \tag{2}$$

with $R_{0\lambda} = \mathrm{Im}(\boldsymbol{\mu}_{0\lambda} \mathbf{m}_{\lambda 0})$ being the rotatory strength for the excitation $0 \rightarrow \lambda$. Here, 0 and λ denote the electronic ground state and one of the excited electronic states of the system under investigation. ω is the frequency of the perturbing field, and the $\omega_{0\lambda}$ are the excitation frequencies (=excitation energies in atomic units). Further, $\boldsymbol{\mu}_{0\lambda}$ and $\mathbf{m}_{\lambda 0}$ are the well-known electric and magnetic transition dipole moment vectors, respectively. We will use atomic units ($\hbar = 1$, $m_e = 1$, $4\pi\varepsilon_0 = 1$, $c \approx 137.036$) throughout this section.

In Ref. 28, we have previously reported TD-DFT expressions for the optical rotation parameter and the rotatory strengths that are consistent with our existing TD-DFT code implementations. The derivation closely follows the previously published approaches for the treatment of frequency-dependent polarizabilities and oscillator strengths.[15,23] A related discussion of this topic can be found in Ref. 29. We summarize the results here for convenience. From an unperturbed, i.e., zeroth-order computation of the molecule under investigation, real Kohn–Sham spin orbitals $\varphi_{i\sigma}$ with occupation numbers $n_{i\sigma}$ (0 or 1 in practice) are available as a basis for the perturbational treatment. The first-order density perturbation due to an external field is then written in the frequency domain as

$$\rho_\sigma'(\mathbf{r},\omega) = \sum_i \sum_a P_{ai\sigma}'(\omega) \varphi_{i\sigma}(\mathbf{r}) \varphi_{a\sigma}(\mathbf{r}) \tag{3}$$

for spin σ. The density matrix P' is specific for the perturbation and represents the computational problem to be solved. We will exclude a possible current-density dependence of the molecular energy here and refer to the literature for details,[12,28,30–35] also with regards to extracting "magnetic information" from the density perturbation within a density matrix-based formalism. Time-independent current-density functional perturbation theory has been applied to magnetic properties, e.g., in Refs. 36 and 37. Numerous applications of DFT to magnetic properties have so far indicated that the neglect of the current-density dependence of the density functional can be a very good approximation for atoms and molecules.

Perturbations of properties described by Eq. (3) are further expressed by using a vector notation based on a composite index ($ai\sigma$) that counts spin–orbital pairs with $n_{a\sigma} < n_{i\sigma}$ (occupied–virtual orbital pairs in practice). According to a common notation, boldface symbols $\mathbf{A},\mathbf{B},\ldots\mathbf{X},\mathbf{Y},\mathbf{Z}$ are used for vectors based on this composite index. We define $X_{ai\sigma} = P_{ai\sigma}'(\omega)$ and $Y_{ai\sigma} = P_{ia\sigma}'(\omega)$. For the first-order electric dipole moment perturbation

$$\mu_u'(\omega) = \sum_{(ai\sigma)} D_{u,ai\sigma}(X_{ai\sigma} + Y_{ai\sigma}) = \mathbf{D}_u \cdot (\mathbf{X} + \mathbf{Y}) \tag{4a}$$

is needed, while for the magnetic moment

$$m_u'(\omega) = \sum_{(ai\sigma)} M_{u,ai\sigma}(X_{ai\sigma} - Y_{ai\sigma}) = \mathbf{M}_u \cdot (\mathbf{X} - \mathbf{Y}) \tag{4b}$$

needs to be used due to the fact that $D_{u,ai\sigma} = D_{u,ia\sigma}$ and $M_{u,ai\sigma} = -M_{u,ia\sigma}$. $\mathbf{D}_u$ and $\mathbf{M}_u$ are here the $(ai\sigma)$ matrix elements of the u component of the electric and magnetic dipole moment operators, $\hat{\mu}_u$ and $-\hat{m}_u$, respectively, in the basis of the unperturbed Kohn–Sham orbitals. Equation (4b) is, in principle, not an approximation since both the time-dependent density and the current density of the noninteracting Kohn–Sham system equal the true time-dependent density and current density, respectively.[7] It is an advantageous

feature of the density matrix-based formalism being employed here that the current density response can be obtained in a simple manner as well.[28,29]

Since for our purpose either the symmetric $(\mathbf{X}+\mathbf{Y})$ or the antisymmetric $(\mathbf{X}-\mathbf{Y})$ part of the perturbation density matrix P', but not $\mathbf{X}$ and $\mathbf{Y}$ individually, is needed, the computational effort can be greatly reduced by solving directly for these quantities. By writing the matrix elements of the frequency-dependent perturbation $\hat{H}'(\omega)$, viz. a component v of a perturbing electric or magnetic dipole field, over the unperturbed Kohn–Sham orbitals as $V_{v,ai\sigma}$ and $W_{v,ai\sigma} = V_{v,ia\sigma}$, and adopting the same vector notation as above, the following equation system can be derived for the desired solutions:[23]

$$(\mathsf{A}+\mathsf{B})(\mathbf{X}+\mathbf{Y})+\omega\mathsf{C}(\mathbf{Y}-\mathbf{X})=\mathbf{V}_v+\mathbf{W}_v\,, \tag{5a}$$

$$(\mathsf{A}-\mathsf{B})(\mathbf{Y}-\mathbf{X})+\omega\mathsf{C}(\mathbf{X}+\mathbf{Y})=\mathbf{W}_v-\mathbf{V}_v\,. \tag{5b}$$

Here, the symbols $\mathsf{A},\mathsf{B},\ldots$, denote matrices based on the composite indices $(ai\sigma)$ and $(bj\tau)$. A, B, and C read explicitly

$$A_{ai\sigma,bj\tau}=\delta_{\sigma\tau}\delta_{ab}\delta_{ij}\frac{\varepsilon_{b\tau}-\varepsilon_{j\tau}}{n_{b\tau}-n_{j\tau}}-K_{ai\sigma,bj\tau}, \tag{6a}$$

$$B_{ai\sigma,bj\tau}=-K_{ai\sigma,jb\tau}, \tag{6b}$$

$$C_{ai\sigma,bj\tau}=\delta_{\sigma\tau}\delta_{ab}\delta_{ij}\frac{1}{n_{b\tau}-n_{j\tau}}. \tag{6c}$$

In case all orbitals have occupation numbers 0 or 1, C is just the negative unit matrix. K is the so-called coupling matrix that describes the first-order response of the molecular Kohn–Sham potential. It is composed of a Coulomb and an exchange-correlation (XC) part

$$K_{ai\sigma,bj\tau}=K^{C}_{ai\sigma,bj\tau}+K^{\mathrm{XC}}_{ai\sigma,bj\tau}, \tag{7}$$

with

$$K^{C}_{ai\sigma,bj\tau}=\int d\mathbf{r}\int d\mathbf{r}' \cdot\varphi^{*}_{a\sigma}(\mathbf{r})\varphi_{i\sigma}(\mathbf{r})\frac{1}{|\mathbf{r}-\mathbf{r}'|}\varphi_{b\tau}(\mathbf{r}')\varphi^{*}_{j\tau}(\mathbf{r}'), \tag{8a}$$

$$K^{\mathrm{XC}}_{ai\sigma,bj\tau}=\int d\mathbf{r}\int d\mathbf{r}' \cdot\varphi^{*}_{a\sigma}(\mathbf{r})\varphi_{i\sigma}(\mathbf{r})f^{\sigma\tau}_{\mathrm{XC}}(\mathbf{r},\mathbf{r}',\omega)\varphi_{b\tau}(\mathbf{r}')\varphi^{*}_{j\tau}(\mathbf{r}'). \tag{8b}$$

$f^{\sigma\tau}_{\mathrm{XC}}(\mathbf{r},\mathbf{r}',\omega)$ is the frequency-dependent exchange-correlation (XC) kernel, i.e., the $t\rightarrow\omega$ Fourier transform of

$$f^{\sigma\tau}_{\mathrm{XC}}(\mathbf{r},\mathbf{r}',t-t')=\frac{\delta V_{\mathrm{XC},\sigma}(\mathbf{r},t)}{\delta\rho_{\tau}(\mathbf{r}',t')}, \tag{8c}$$

with $V_{\mathrm{XC},\sigma}$ being the XC potential for spin σ. For practical purposes we will assume usage of the static (adiabatic, no memory effects) limit of $f^{\sigma\tau}_{\mathrm{XC}}(\mathbf{r},\mathbf{r}',\omega)$ within a simple local density approximation (LDA), i.e., the ALDA XC kernel. This makes the coupling matrix ω independent.

An expression for β_{uv}, from which the rotatory strengths are obtained, can now be derived in a straightforward manner either from (4a), where $(\mathbf{X}+\mathbf{Y})$ is due to a perturbation by an external magnetic field, or from (4b), where $(\mathbf{X}-\mathbf{Y})$ is due to the perturbation by an external electric field. We refer the reader to Ref. 28 for details. From (4b), e.g., one obtains

$$\beta_{uv}=2c\,\mathrm{Im}(\mathbf{D}_u\mathsf{S}^{-1/2}[\omega^2-\Omega]^{-1}\mathsf{S}^{1/2}\mathsf{C}^{-1}\mathbf{M}_v), \tag{9}$$

with the diagonal matrix S

$$\mathsf{S}=-\mathsf{C}(\mathsf{A}-\mathsf{B})^{-1}\mathsf{C}, \tag{10}$$

and the Hermitian matrix Ω

$$\Omega=-\mathsf{S}^{-1/2}(\mathsf{A}+\mathsf{B})\mathsf{S}^{-1/2}. \tag{11}$$

Following the lines of Ref. 23, the inverse of $[\omega^2-\Omega]$ is further expressed in the form of its spectral resolution, with $\mathbf{F}_{0\lambda}$ being the eigenvectors of Ω

$$[\omega^2-\Omega]^{-1}=-\sum_{\lambda}\frac{\mathbf{F}_{0\lambda}\otimes\mathbf{F}_{0\lambda}}{\omega^2_{0\lambda}-\omega^2}. \tag{12}$$

This allows one to identify the solutions $\omega^2_{0\lambda}$ of the pseudo-eigenvalue problem

$$\Omega\mathbf{F}_{0\lambda}=\omega^2_{0\lambda}\mathbf{F}_{0\lambda}\,, \tag{13}$$

with the squares of the excitation energies $\omega_{0\lambda}$ of the system under investigation. Substitution of (12) in (9) discloses the connection of Eq. (9) with the SOS expression for β_{uv}. By comparison with Eq. (2), the rotatory strengths of the transitions are given by

$$R_{0\lambda}=\mathrm{Im}\left(\sum_{u}\mathbf{D}_u\mathsf{S}^{-1/2}\mathbf{F}_{0\lambda}\cdot\mathbf{F}_{0\lambda}\mathsf{S}^{1/2}\mathsf{C}^{-1}\mathbf{M}_u\right). \tag{14}$$

From that, a component of the electric transition dipole moment $\mu_{u,0\lambda}$ will be identified with

$$\mu_{u,0\lambda}=\omega^{-1/2}_{0\lambda}\mathbf{D}_u\mathsf{S}^{-1/2}\mathbf{F}_{0\lambda}\,. \tag{15a}$$

It is necessary to include the factor of $\omega^{-1/2}_{0\lambda}$ in (15a) in order to yield a consistent expression for the transition dipole moments as compared to a similar treatment of the frequency-dependent polarizability.[23] Thus, a component of the magnetic transition dipole moment $\mathbf{m}_{0\lambda}$ reads

$$m_{u,0\lambda}=-\omega^{1/2}_{0\lambda}\mathbf{M}_u\mathsf{C}^{-1}\mathsf{S}^{1/2}\mathbf{F}_{0\lambda}\,, \tag{15b}$$

where the minus sign has been included because the expression for $R_{0\lambda}$, Eq. (2), contains $\mathbf{m}_{\lambda 0}$, and $\mathrm{Im}(\boldsymbol{\mu}_{0\lambda}\mathbf{m}_{\lambda 0}) = -\mathrm{Im}(\boldsymbol{\mu}_{0\lambda}\mathbf{m}_{0\lambda})$. The expression (15b) can also directly be obtained from a TD-DFT expression for the paramagnetic susceptibility, and comparison with the corresponding SOS formula, by considering the perturbation of the magnetic moment by a time-dependent magnetic field.[28] As already noted in Ref. 23, the formalism employed here is technically related to the time-dependent Hartree–Fock or random phase approximation (RPA) method.[38,39] A corresponding RPA treatment of chiroptical properties was discussed, e.g., in Refs. 4, 40.

The practical aspects of this work are concerned with circular dichroism. The solutions of Eq. (13) as well as the quantities $\mathbf{M}_u$, $\mathbf{D}_u$, S (and C, which is the unit matrix in

practice) are needed in order to compute the rotatory strengths. The implementation of solving Eq. (13) based on the efficient use of symmetry-adapted numerical integration and auxiliary density fit functions has already been carried out and is extensively described in Refs. 16 and 41. The program code forms part of the RESPONSE module of the Amsterdam Density Functional program system (ADF). We have extended this code for the computation of the matrix elements $\mathbf{M}_u$ and the rotatory strengths $R_{0\lambda}$ based on Eq. (14). Further, in order to be able to obtain origin-independent rotatory strengths, and to better assess the quality of the results, the dipole-velocity form for the electric transition dipole moments

$$\mu^{\nabla}_{u,0\lambda} = -\omega_{0\lambda}^{-1/2} \boldsymbol{\nabla}_u \mathsf{C}^{-1} \mathsf{S}^{1/2} \mathbf{F}_{0\lambda}, \tag{16}$$

has been implemented in the RESPONSE module as well. Here, $\boldsymbol{\nabla}_u$ denote the $(ai\sigma)$ matrix elements of the operator $-\partial/\partial u$. As can be easily seen from (16) and (15b), any contribution to $R_{0\lambda}$ due to a displacement of the molecule will automatically vanish when (16) is used instead of (15a) regardless of the quality of the basis. In principle, origin-independent rotatory strengths based on the dipole-length formula can be computed by employing so-called gauge-including or gauge-independent atomic orbitals (GIAOs). See Ref. 42 for a corresponding RPA implementation. However, the accurate determination of excitation energies demands rather large basis sets. We have found that with these basis sets, the dipole velocity form (16) of $\boldsymbol{\mu}_{0\lambda}$ systematically agrees very well with the result obtained from the dipole-length form, and therefore accurate, origin-independent rotatory strengths are obtained without the need to employ GIAOs. Pragmatically speaking, though it is desirable to have a GIAO implementation of rotatory strengths, in practice, CD spectra simulated with small basis sets are questionable, while with large basis sets the dipole-velocity formula can alternatively be employed. Currently, apart from the trivial C_1 case, the most important chiral symmetry groups C_2 and D_2 are supported for the CD spectra computation. For these cases, the already available symmetry-related part of the numerical integration code can be employed without modifications, since *x, y, z* and the rotations R_x, R_y, R_z, respectively, belong to the same (one-dimensional) irreducible representations and can therefore be treated on an equal footing.

III. COMPUTATIONAL DETAILS

Computations of singlet excitation energies, oscillator strengths, and rotatory strengths have been carried out with a modified version of the AMSTERDAM DENSITY FUNCTIONAL program (ADF).[17–20] Previously reported Slater basis sets suitable for the treatment of excitation energies were employed in most cases. These basis sets are derived from the triple-ζ doubly polarized standard ADF basis "V," and contain additional diffuse functions. We will label this basis as "Vdiff" in the following. Since there is no basis set for Cl available in Vdiff, a recently developed even-tempered, all-electron basis has been used for the chloro-aziridines (denoted "VIdiff"), with $7s$, $5p$, $3d$, and $2f$ functions for C, $9s$, $7p$, $4d$, and $2f$ functions for Cl, and $5s$, $3p$, and $2d$ for H and $\zeta_{n+1}/\zeta_n = 1.7$. For the methyloxiranes, both Vdiff and VIdiff were found to yield almost identical results and are thus of comparable quality. The Vdiff basis sets have been confirmed to yield reliable excitation energies and response properties. See Refs. 15, 17, 43, and 44 for details. For the helicenes, the much smaller triple-ζ singly polarized ADF basis "IV" without diffuse functions resulted in favorable agreement with previous TD-DFT computations by other authors for the simulated CD spectra. Very similar results to the ones with basis IV have been obtained by us for the helicenes with the even smaller double-ζ singly polarized basis "III" (not reported in this work). The quality of the basis sets with respect to the desired properties can be assessed by a comparison of the dipole-length and dipole-velocity representation of the oscillator strengths and rotatory strengths. For rotatory strengths, the deviations were typically smaller than 5% for the helicenes and smaller than 1%–2% for the small molecules for which the "diff" basis sets could be employed. Results referring to the dipole-length representation are reported here.

As already mentioned, Ω in Eq. (13) is based upon the ALDA XC kernel in all computations. This affects the quality of the first-order Kohn–Sham potential induced by the perturbation due to the external field. This is to be distinguished from the zeroth-order Kohn–Sham potential that is being used in order to determine the unperturbed orbitals and orbital energies. It has been demonstrated[44] by comparison to highly accurate ("exact") Kohn–Sham potentials that approximations to the zeroth-order Kohn–Sham potential, on which the unperturbed orbitals and orbital energies depend, significantly affect the results, while the ALDA approximation for the kernel appears to be excellent. See also Refs. 9 and 45. Here, we have applied four different functionals for the zeroth-order potential: the well-known local density approximation (LDA) in form of the Vosko–Wilk–Nusair[46] (VWN) functional, VWN+gradient corrections (GGA) in the form of the popular Becke88–Perdew86 ("BP86") functional,[47–49] and further, the "statistical average of orbital potentials" potential (SAOP) by Gritsenko, Baerends *et al.*[24] and the "gradient-regulated connection" (GRAC) potential.[25] These potentials have been developed specifically with the accuracy of excitation energies and response properties in mind. The GRAC potential requires the ionization potential as input. The experimental data from Ref. 50 were used for methyloxirane and *trans*-dimethyloxirane for this purpose. Both SAOP and GRAC correct the Kohn–Sham potential in particular in the outer "asymptotic" region and thus lead to much improved virtual orbitals and virtual orbital energies as compared to standard LDA or GGA potentials. This has been shown to significantly improve excitation energies and frequency-dependent polarizabilities in DFT calculations.[24,25]

The Davidson algorithm has been employed to obtain a number of low-lying singlet excitations instead of solving the full problem of Eq. (13). Details of the ADF implementation are summarized in Refs. 16 and 41. The "linear scaling" and parallelization features available with ADF[41] have not been employed in this work, but no principal features of our

TABLE I. Electronic excitations in (R)-methyloxirane. Excitation energies E in eV, rotatory strengths R in 10^{-40} c.g.s. units, oscillator strengths f in 10^{-3} a.u. R and f based on dipole-length representation of $\boldsymbol{\mu}_{0\lambda}$.

#		LDA[a]	GGA[a]	SAOP[a]	GRAC[a]	LDA[b]	MRCI[c]	HF[d]	Expt.[e]	Expt.[f]
1	E	5.93	6.05	7.11	6.46	6.0	6.25	6.40	7.07	7.12
	f	12.0	11.0	13.0	11.5	12.0		0.4		25.0
	R	−22.8	−20.1	−26.7	−24.4	−23.0	−6.43	−2.66	−12.6	−11.8
2–4	$\overline{E}$	6.48	6.58	7.69	7.05	6.5	6.95	7.3	7.70	7.75
	Σf	49.0	46.0	61.0	59.5	44.0		1.2		62.0
	ΣR	22.2	19.1	29.5	25.1	23.0	7.93	2.24	6.98	10.8

[a]TD-DFT, this work, basis "Vdiff."
[b]TD-DFT, numerical approach, Ref. 4.
[c]Multireference configuration interaction (singles+doubles), Ref. 51.
[d]Hartree–Fock, Δ-SCF, Ref. 57.
[e]Reference 51, combined theor./expt. study.
[f]Reference 57, combined theor./expt. study.

code restrict the use of them in order to study very large systems.

For methyloxirane and the helicenes, previously reported Hartree–Fock optimized geometries were taken from Refs. 12 and 51 in order to allow for a direct comparison of the rotatory strengths with computational data in the literature. In all other cases, B3LYP/6-311G** optimized structures have been used. Rotatory strengths are reported in the usual c.g.s. units of 10^{-40} esu·cm·erg/G, where 1 esu·cm·erg/G corresponds to $\approx 3.336 \cdot 10^{-15}$ C·m·J/T in SI units. Following previous computational studies of the CD effect, the simulation of CD spectra is based on the relation

$$R_{0\lambda} = 22.97 \int_{\text{CD band } \lambda} dE \cdot \frac{\Delta\epsilon(E)}{E}, \tag{17}$$

where $R_{0\lambda}$ is in 10^{-40} c.g.s. units, the difference in the absorption coefficients for left- and right-hand circular polarized light, $\Delta\epsilon$, is in 1/(mol cm), and E is in eV. See, e.g., Refs. 52–55. For each computed excitation, a normalized Gaussian centered at the excitation energy is scaled so as to reproduce the computed $R_{0\lambda}$ by Eq. (17). The plotted theoretical "CD spectrum" is then obtained as the superposition of all these Gaussian curves. Unless otherwise noted, for the linewidth ΔE, we employ the empirical recipe proposed by Brown *et al.* in Ref. 53, viz., $\Delta E \approx 0.08\sqrt{E}$ with E in eV. In case this estimate did not reproduce enough details in the simulated spectrum, a somewhat smaller coefficient between 0.05 and 0.08 has been used instead. We have to stress that this procedure does not involve a theoretical treatment of line shapes and-widths. The linewidths are used here as adjustable parameters in order to mimic a real spectrum. This often yields simulated spectra that look very similar to the experimental ones. Important corrections to the excitation energies and the form of the CD bands arising from solvent effects or molecular vibrations are currently neglected.

IV. RESULTS AND DISCUSSION

A. (R)-Methyloxirane

The rotatory strengths for the first four singlet excitations of (R)-methyloxirane have been computed in order to perform a first practical test of our implementation. This is one of the smallest molecules for which experimental and theoretical data are available for comparison. Its modest size allows for the use of rather large basis sets, high numerical integration accuracy, and tight convergence criteria and the neglect of cutoff features. At the same time, the transitions in methyloxirane are already a rather challenging problem since the lowest transitions are Rydberg excitations that require diffuse basis functions and an accurate Kohn–Sham potential. Our results are presented in Table I together with data previously published by other authors. In particular, the agreement with the fully numerical TD-DFT study of Ref. 14 for the LDA functional is very good. However, these results do not compare well with experimental data. In conjunction with other theoretical results, Table I illustrates that it is rather difficult to obtain accurate rotatory strengths both theoretically and experimentally. In the light of these restrictions, the agreement of our results with the experimental estimates can be regarded as satisfactory.

It is already known from previous studies that the first four transitions in methyloxirane are excitations from the HOMO, dominantly located around the oxygen, into s and p Rydberg states. All listed theoretical and experimental data agree in so far that the lowest (HOMO→s) transition has a negative rotatory strength for (R)-methyloxirane, while the sum of the rotatory strengths for the next three transitions (HOMO→p) is of opposite sign and has approximately the same magnitude. However, the actual values differ by up to a factor of 10. In the perturbational CI study of Rauk,[56] signs for the rotatory strengths opposite to those listed in Table I have been reported. Therefore, these data are not included in the table. The deficient results have been attributed by Rauk to the importance of reorganization of the "unexcited" electrons upon excitation, which could not be properly described by the method being used in Ref. 56. This appeared to be the case in particular for the first transition of methyloxirane. The quoted results of Ref. 57 do not seem to be very reliable since large deviations between the dipole-length and dipole-velocity representations of R and f were observed there. However, the signs of R were obtained correctly. From our computations we find, e.g., for the GGA results oscillator strengths of 0.011 and 0.046 for excitations numbers 1 and 2–4, and rotatory strengths of −20.3 and 19.3, respectively,

TABLE II. Electronic excitations in *trans*-(2S,3S)-dimethyloxirane. Excitation energies E in eV, rotatory strengths R in 10^{-40} c.g.s. units, oscillator stregths f 10^{-3} a.u. R and f based on dipole-length representation of $\boldsymbol{\mu}_{0\lambda}$.

#		GGA[a]	SAOP[a]	GRAC[a]	MRCI[b]	HF[c]	Expt.[d]	Expt.[e]
1*B*	*E*	5.86	6.92	6.28	6.72	6.36	6.97	7.06
	f	12.4	11.1	12.6	11.6	0.5	···	20
	R	10.3	15.0	15.5	7.63	3.04	9.48	20
1*A*	*E*	6.20	7.26	6.63	7.05	6.64	7.35	7.45
	f	0.12	0.08	0.002	11.2	1.3	···	···
	R	5.17	2.28	−0.36	−10.8	−4.1	−0.13	−0.4
2*A*	*E*	6.33	7.42	6.79	7.44	7.18	7.56	7.74
	f	11.1	19.3	15.2	0.6	0.4	···	50
	R	−16.2	4.64	−13.2	1.44	0.42	6.18	14
2*B*	*E*	6.61	7.76	7.24	7.20	7.08		
	f	10.3	17.5	14.0	12.7	0.5		
	R	12.5	−17.6	16.3	5.65	0.74		

[a]TD-DFT, this work, basis "Vdiff."
[b]Multireference configuration interaction (singles+doubles), Ref. 58.
[c]Hartree–Fock, Δ-SCF, Ref. 57.
[d]Reference 58.
[e]Reference 57.
[f]Experimental data for average (excitation energies) and sum (rotatory strength) of 2*A* and 2*B*.

obtained with the dipole-velocity form of $\boldsymbol{\mu}_{0\lambda}$, which are in good agreement with the dipole-length values of Table I.

From a comparison of our data obtained with different density functionals, it can be seen that with the standard LDA or GGA functionals for this particular system the excitations energies are systematically underestimated by more than 1 eV. The SAOP potential yields greatly improved excitation energies here, which favorably agree with the experimental values. The GRAC potential offers a clear improvement over LDA and GGA, but appears to be less accurate than SAOP in this case. However, the oscillator strengths are of comparable quality with all four methods, the sum of transitions 2–4 being slightly better reproduced by SAOP and GRAC as compared to LDA and GGA. For the rotatory strengths, the results obtained with the SAOP potential seem to be slightly less accurate than the LDA, GGA, and GRAC values if compared to experiment, but overall approximately the same accuracy is achieved for the rotatory strengths as well. It is known that with standard LDA or GGA functionals the energy differences between the occupied and virtual orbitals, as a zeroth-order estimate of the excitation energies in our perturbational treatment, are often too small. Since these energy differences enter the expression for $\boldsymbol{\Omega}$ in Eq. (13), excitation energies are often systematically underestimated with standard LDA and GGA functionals. Potentials such as GRAC and SAOP have been designed in order to overcome this limitation regarding the computation of excitation energies. These potentials at the same time alter the shape in particular of the virtual orbitals. This, of course, affects the matrix elements **D** and **M** entering the expressions for the rotatory strengths, and also the sensitive solutions $\mathbf{F}_{0\lambda}$ of Eq. (13). In combination, and depending on the actual system, individual rotatory strengths might not inevitably be expected to improve when compared to experiment, even though the excitation energies are systematically improved. However, these potentials have been found to lead to superior results for response properties as well,[24,25] indicating that the orbital shapes are altered in conjunction with the orbital energies in a physically meaningful way. We will therefore see in the following that the SAOP and GRAC potentials usually lead to an enhanced accuracy for individual rotatory strengths as well.

B. *Trans*-2,3-dimethyloxirane

The CD spectrum of *trans*-2,3-dimethyloxirane has been previously studied experimentally and theoretically by, e.g., Carnell *et al.*[58] and Cohen *et al.*[57] The molecule has C_2 symmetry, which allows us to employ symmetry in the TD-DFT computations. The computations including or excluding symmetry and use of the symmetry-adapted integration grid were confirmed to yield the same results within the numerical accuracy. A comparison of our data with other theoretical and experimental estimates is listed in Table II.

The data shows that the signs of the rotatory strength of the first transition ($n\rightarrow 3s$) agree for all theoretical and experimental values. As for methyloxirane, the GRAC and SAOP potentials yield larger R values than the GGA functional, but all of them compare favorably with the experimental data. The GGA functional underestimates the excitation energies by about 1.1 eV, while the SAOP potential reproduces the experimental values to a very good agreement. Again, GRAC leads to less of an improvement than SAOP. The group of transitions #2–4 is close in energy, and our TD-DFT computations predict a different sequence for the ± sign pattern of the rotatory strengths than that predicted by the *ab initio* computations. Also, the energetic ordering of the 2*A* and 2*B* transitions is opposite with TD-DFT than what has been obtained with the *ab initio* methods. Unfortunately, the experimental spectra do not allow for a clear distinction between these 3 CD bands since they strongly overlap and cancel to a large extent due to their opposite signs. The sum of rotatory strengths for the three $n\rightarrow 3p$ Rydberg transitions is 1.47 for GGA, 2.74 for GRAC,

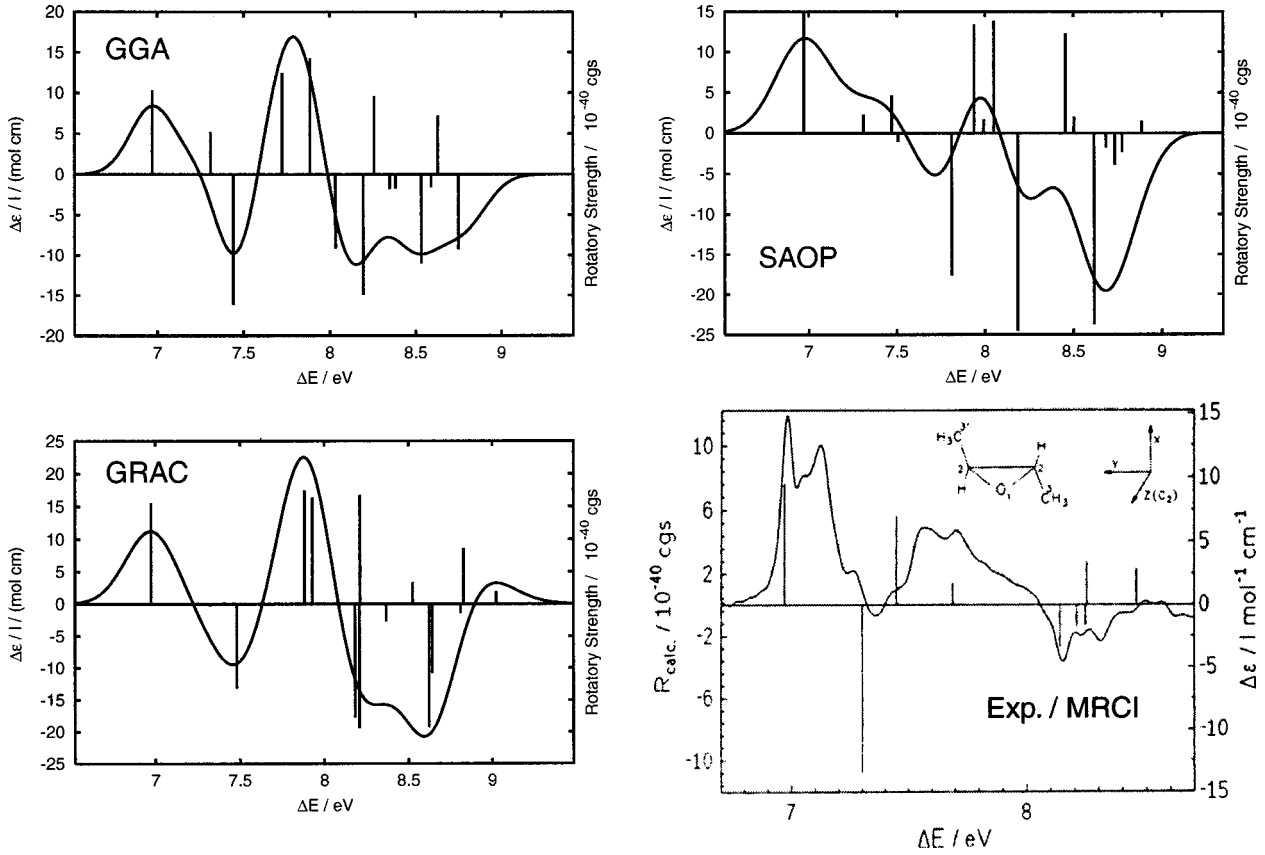

FIG. 1. Simulated and experimental CD spectra of *trans*-(2S, 3S)-dimethyloxirane. The spectra based on GGA, GRAC, and SAOP are blueshifted by 1.11, 0.69, and 0.05 eV, respectively, such that the first transition coincides with the experimental value of 6.97 eV. Experimental spectrum and MRCI rotary strengths from Ref. 58, © (1994), reprinted with permission from Elsevier Science.

and −10.68 for SAOP, respectively, as compared to −3.71 from the MRCI study, −2.94 from the HF study, and 6.05 and 13.6 from the experiments. Clearly, the agreement between different theoretical approaches and experiments is not as good as for the case of methyloxirane due to the cancellation of large positive and negative numbers and also rather large error bars for the rotatory strengths extracted from the spectra.

Figure 1 shows the simulated CD spectra from our computations in comparison to the experimental spectrum of Ref. 58. The TD-DFT simulations reproduce the overall shape of the spectrum with regards to its sign pattern rather well. With an estimated linewidth of ~0.1 eV for the first CD band, the experimental $\Delta\epsilon$ value is reproduced quite accurately. The high-lying CD bands are strongly overestimated in magnitude by the TD-DFT simulations, but the overall shape of the spectrum is reasonably well reproduced. The authors of Ref. 58 have reported increasing magnitudes of the rotatory strengths with increasing quality of the CI wave functions employed in their work, which somewhat supports our findings since we can expect an overestimation of the strengths of the respective CD bands, as compared to experiment, in the TD-DFT computations as well. According to our calculations listed in Table II, one of the $n\rightarrow 3p$ transitions has a very large negative rotatory strength that leads to a negative CD band in the simulated CD spectra at about 7.3 to 7.5 eV but is not observed experimentally. In the SAOP case, the position of this transition is shifted to higher energy which leads to a better agreement of the shape of the spectrum with experiment in the low-energy range but yields a slightly blueshifted positive CD band at about 8 eV, which should occur rather around 7.7 eV. The spectra based on GGA and GRAC, on the other hand, are somewhat obscured in the lower energy range due to the presence of the aforementioned large negative CD band. It remains an open question why the computations and experiments do not agree regarding this large negative rotatory strength.

C. Cyclohexanone derivatives

The lowest transition arising from the carbonyl chromophore of cyclohexanone derivatives has in particular been the subject of pioneering studies of computational CD. Moscowitz[2,59] has computed experimental rotatory strengths for a number of cyclohexanones from their respective ORD spectra. Error estimates of these values were not given. His semiempirical approach for rotatory strengths was parametrized with these data for a subset of a number of structurally related cyclic ketones, which then yielded excellent agreement for the remaining compounds. Other studies with semiempirical[60] or extended Hückel[61] wave functions that were not specifically parametrized for reproducing a single rotatory strength did not yield such excellent agreement. In particular, the extended Hückel treatment did not allow for a quantitative estimate since the rotatory strengths were systematically too large in magnitude. Noting the frequent dis-

TABLE III. Rotatory strengths R of the C═O $n-\pi^*$ transition of substituted cyclohexanones, in 10^{-40} c.g.s. units. R is based on dipole-length representation of $\boldsymbol{\mu}_{0\lambda}$.

H→CH$_3$[a]	GGA[b]	SAOP[c]	EH[d]	CNDO[e]	Expt.[f]
H_7	0.12	0.47	9.19	0.00	+small
H_8	3.65	5.54	5.52	3.25	
H_9	(1.57)	−1.27	−13.99	−2.09	−[g]
H_{10}	(−0.78)	0.47	4.85	2.18	
H_7H_{13}	(−3.7)	1.00	5.12	3.3	1.7
$H_7H_{13}H_8$	2.15	9.08	5.88	4.9	6.2

[a]Index of hydrogen substituted by methyl; see the text.
[b]TD-DFT, this work, basis "Vdiff." With GGA and the diffuse basis sets, sometimes only moderate SCF convergence could be achieved, indicated by numbers in parentheses.
[c]TD-DFT, this work, basis "Vdiff."
[d]Extended Hückel, idealized geometries, Ref. 61.
[e]Semiempirical CNDO wave function, idealized geometries, Ref. 60.
[f]Experimental data by Moscowitz, Ref. 2.
[g]Magnitude not known.

cussion of the CD effect for methyl-substituted cyclohexanones in chemistry textbooks and its rationalization by the "octant rule,"[62] not very many first-principle studies are available.[5] Table III displays the results of the two previously mentioned studies together with our TD-DFT data (GGA and SAOP) for the 290 nm $n-\pi^*$ transition of the carbonyl chromophore for these molecules. The labeling of the hydrogens has been chosen as follows:

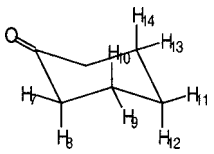

Excitation energies are not listed in Table III since they hardly change among the series of molecules. The experimental value is approximately 4.4 eV, GGA: 3.9–4.1, SAOP: 4.3–4.4 eV. As already noted in Refs. 24 and 25 the SAOP potential yields a substantial improvement in particular for Rydberg states, but only minor improvements for valence excitations for which GGA functionals already perform rather well. However, even though the transitions are not of Rydberg type, we have used the same basis set "Vdiff" as for the oxiranes. With the smaller basis "V" that does not contain diffuse functions, we have found poor agreement between the rotatory strengths obtained from the dipole-length and dipole-velocity forms, while the deviations are less than 5% for the larger basis.

Even though GGA and SAOP yield very similar excitation energies Table III shows that the rotatory strengths for the lowest excitation of the ketones differ substantially. In some cases, only moderate self-consistent field (SCF) convergence could be achieved with the GGA functional and basis Vdiff, and the computed Rs have the sign opposite the SAOP values. For the other cases, signs and relative magnitudes of the rotatory strengths as compared to the experimental estimates by Moscowitz are reasonable. Unlike other cases mentioned in the literature,[52] for which the computed rotatory strengths do not seem to depend strongly on the chosen geometry, we find that this is not the case for the samples here. Employing the idealized geometries of Refs. 60 and 61 (on which the EH and CNDO values in Table III are based) as well as the smaller basis V together with the GGA functional did in fact yield favorable TD-DFT rotatory strengths of the same sign and similar magnitude to the ones obtained in Ref. 60 and the experimental estimates. However, R values based on optimized geometries but otherwise the same computational settings resulted in no agreement of signs and magnitudes for both GGA and SAOP with reference values. Only the use of the larger basis Vdiff again yielded reasonable results, at least for SAOP (Table III). We decided to show the values according to the optimized geometries. Our findings may be rationalized by noting that substitution of the equatorial hydrogens, or those far away from the carbonyl group, by methyl groups, and keeping the symmetric ring structure fixed, imposes only a minor chiral perturbation with respect to the C═O n and π^* orbital. The equatorial methyl carbons lie in or very close to the nodal plane of the π^*; therefore, the perturbation is largely due to the methyl hydrogens (the methyl groups will also be freely rotating in the experiments). Using optimized geometries, new contributions from other, now slightly displaced atoms also occur, and the final result consists of contributions of opposite sign from several dissymmetries in the neighborhood of the C═O group. Taking this into account, it does not seem unreasonable that the sign of the rotatory strengths for the H_7 and H_9 substituted cyclohexanone can change upon small changes of the orbitals (GGA versus SAOP or only modest vs tight SCF convergence). For the clear-cut cases where the methyl substitution of H_8 causes a large effect, all computations listed in Table III agree with respect to their signs.

D. Aziridines

The CD spectra of aziridine derivatives have been subject to previous computational studies.[56,63] As an example we provide here the TD-DFT CD spectra simulation of (1R,2S)-1-chloro-2-methyl-aziridine (CMA1a), (1S,2S)-1-chloro-2-methyl-aziridine (CMA1b), and (+)-1-chloro-2,2-dimethylaziridine (CDMA); see Fig. 2. The rotatory strengths for the lowest two transitions for our TD-DFT computations and the earlier experimental/CI study of Shustov *et al.*[63] are displayed in Table IV. The linewidths were set to approximately 0.2 eV, leading to a favorable agreement of the magnitudes of $\Delta\varepsilon$ for the first (lowest energy) CD band of CMA1a with the experimental spectrum. With this linewidth, the magnitude of $\Delta\varepsilon$ for CMA1b is also well reproduced, as well as the zeros at about 240 nm for CMA1a and CDMA. The simulated spectra suggest that the blueshift of the first CD band of CMA1b as compared to CMA1a might be due to a lower experimental resolution that causes the first two CD bands of CMA1b to appear as one, shifted to higher energy. Likewise, the very small rotatory strength of the first CD band of CDMA could be due to overlapping bands of opposite sign in the experimental spectrum (please note that the experimental CD spectrum of CDMA is magnified by a factor of 10 in Fig. 2).

Comparing GGA and SAOP for these molecules, we find that the computed excitation energies are of comparable accuracy. Both potentials underestimate the lowest excitation

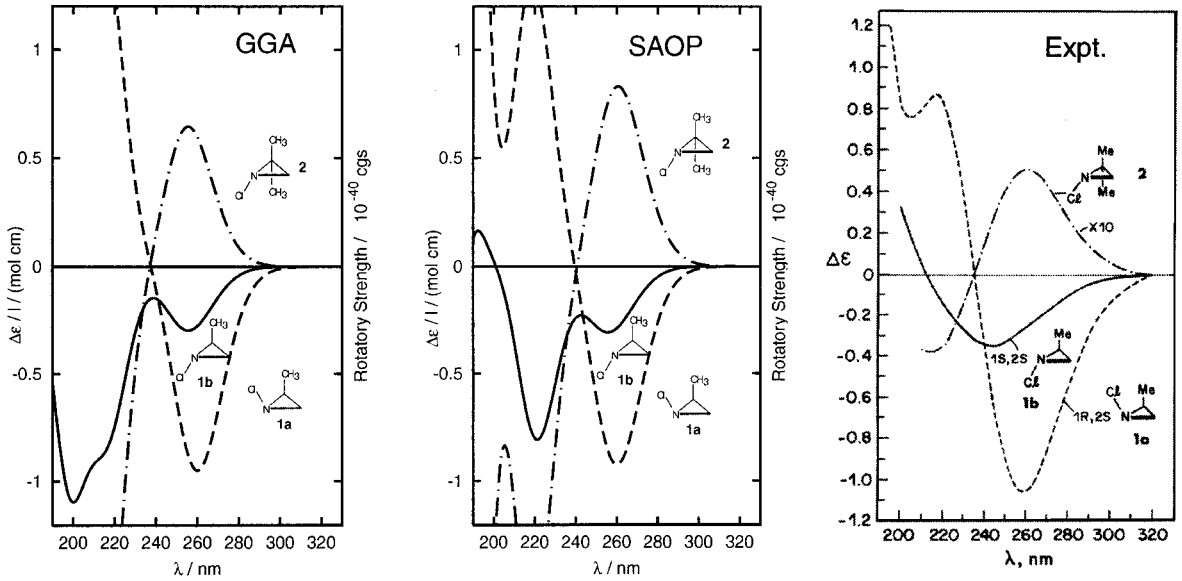

FIG. 2. Simulated and experimental CD spectra of (1R, 2S)-1-chloro-2-methyl-aziridine (1**a**), (1S, 2S)-1-chloro-2-methyl-aziridine (1**b**), and (+)-1-chloro-2, 2-dimethylaziridine (2). The simulated spectra are blueshifted by 0.67 and 0.52 eV for GGA and SAOP, respectively, such that the first transition for 1a coincides with the experimental value of 260 nm. Please note that the experimental spectrum of **2** is magnified by a factor of 10. Experimental spectrum reprinted with permission from Ref. 63, © (1988) American Chemical Society.

energies by approximately one half of an eV, with SAOP performing only slightly better. The resulting rotatory strengths of the first two transition have similar magnitude with both methods. They also agree reasonably well with the *ab initio* data of Ref. 63.

E. Helicenes

The [n]-helicenes are highly interesting screw-shaped model compounds that exhibit huge optical rotations. Much has been learned about optical activity by studying the OR and CD of these compounds. As already stated in Ref. 12, hexahelicene ''is the paradigm of the helically chiral molecule.'' In this work, the authors have (re-)investigated the CD spectra of a number of substituted and unsubstituted helicenes experimentally and by time-dependent DFT (BP86), based on their implementation in the TURBOMOLE program. A related study of helicenes was previously published by Grimme *et al.*[64] based on an approximation to TD-DFT. Pioneering experimental and theoretical work has been carried out by Mason *et al.*[53,54]

TABLE IV. Rotatory strengths of the lowest two transitions of methyl substituted chloro-aziridines, in 10^{-40} c.g.s units. *R* is based on dipole-length representation of $\boldsymbol{\mu}_{0\lambda}$.

Molecule[a]		GGA[b]	SAOP[c]	CI-PT[d]	Expt.[e]
CMA1a	λ/nm	302	292	213	260
	R	−2.82	−2.71	−4.0	
	λ/nm	244	241	178	216
	R	3.52	3.52	0.9	
CMA1b	λ/nm	297	288	208	244
	R	−0.87	−0.88	−0.5	
	λ/nm	246	244	179	···
	R	−1.96	−2.16	−1.2	
CDMA	λ/nm	297	293	···	260
	R	1.90	2.43		
	λ/nm	244	241	···	217
	R	−4.41	−4.49		

[a]See the text for definition of acronyms.
[b]TD-DFT, this work, basis ''VIdiff.''
[c]TD-DFT, this work, basis ''VIdiff.''
[d]CI perturbation study of Ref. 63.
[e]In heptane, Ref. 63. *R* not determined.

We do not attempt to repeat the detailed discussion of the spectra and the analysis of Ref. 12, and earlier work, here. However, the availability of TD-DFT simulated spectra allows us to make a direct comparison between the different codes and approaches [e.g., the use of Gaussian basis sets in Ref. 12 versus Slater-type functions in this work, different implementations of the algorithms to solve Eq. (13), etc.]. Penta- and hexahelicene have been chosen for the comparison. We have used the molecular geometries reported in Ref. 65, which have also been used in Ref. 12. A set of two diffuse *s* and *p* functions, respectively, has been placed between the benzene rings or in the ring centers to allow for a description of low-lying Rydberg excitations. The C_2 symmetry of the helicenes has been employed in the computations. See Sec. III for further details. The resulting simulated spectra are displayed together with the spectra of Ref. 12 in Figs. 3 and 4. All theoretical spectra are blueshifted by 0.45 eV. We used a constant linewidth of 0.1 eV here.

Additionally, a computation for hexahelicene has been carried out with the basis set Vdiff and the SAOP functional. The shape of the corresponding spectrum is practically the same as the one obtained with GGA and the basis set IV and therefore not displayed. Moreover, the spectrum needs to be blueshifted by 0.45 eV as well in order to yield agreement of the positions of the CD bands with the experimental spectrum. We thus conclude that the underestimation of the TD-DFT excitation energies in this case is not due to basis set limitations or deficient DFT potentials, but rather due to the neglect of other factors that influence the experimental spec-

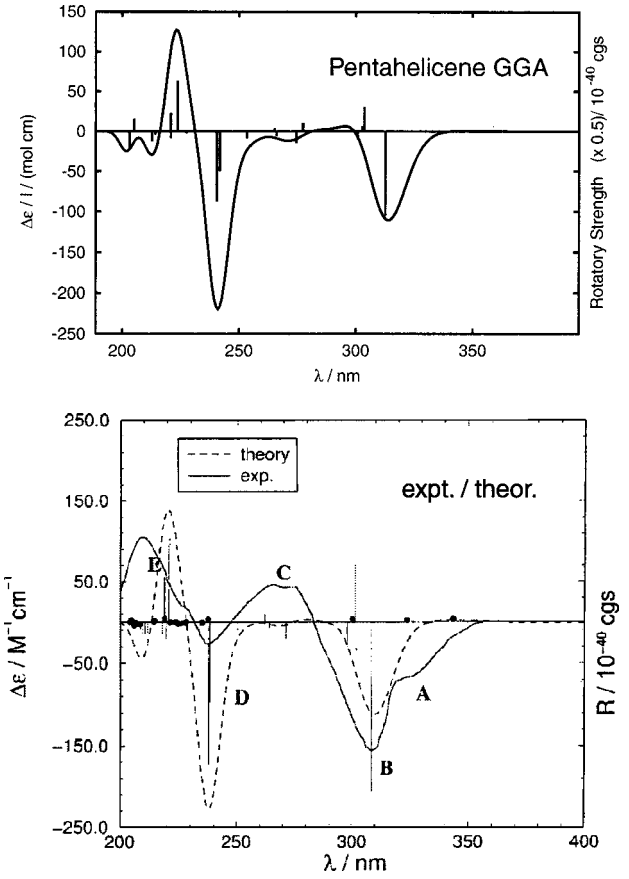

FIG. 3. Simulated and experimental/theoretical CD spectra of (M)-pentahelicene. The theoretical spectra are blueshifted by 0.45 eV. Experimental and simulated TD-DFT spectrum reprinted with permission from Ref. 12, © (2000) American Chemical Society.

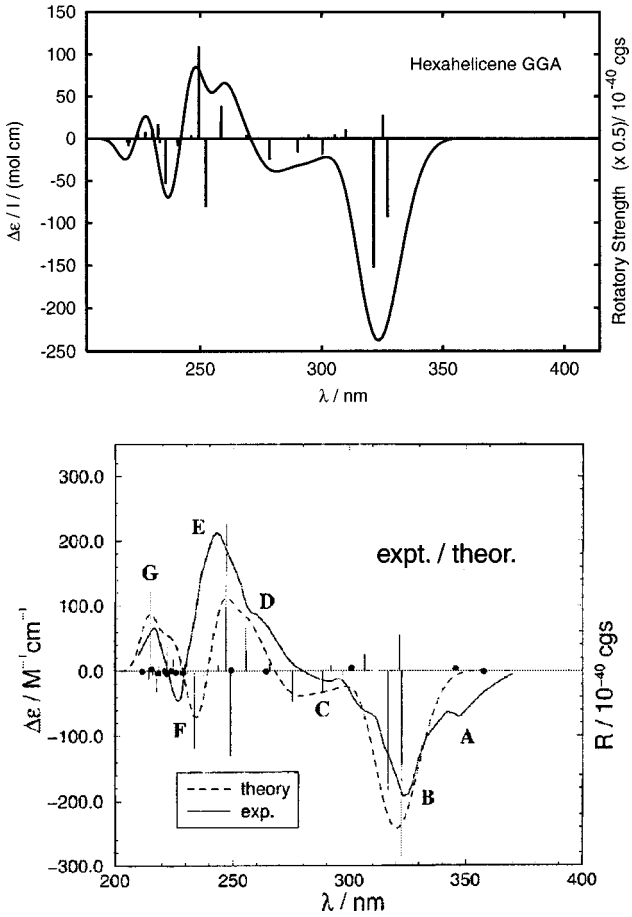

FIG. 4. Simulated and experimental/theoretical CD spectra of (M)-hexahelicene. The theoretical spectra are blueshifted by 0.45 eV. Experimental and simulated TD-DFT spectrum reprinted with permission from Ref. 12, © (2000) American Chemical Society.

trum, most notably, solvent effects. Besides this, the agreement between our simulated TD-DFT spectra and the ones from Ref. 12 is excellent. Both the general shape of the spectra as well as excitation energies and rotatory strengths of individual transitions are very similar, as can be expected since the underlying theoretical approach [solution of Eq. (13)] and the chosen functional (BP86) are the same and the basis sets are of comparable quality with respect to excitation energies.

V. SUMMARY

We have implemented a method in the RESPONSE module of the ADF program that makes it possible to calculate the rotatory strengths for electronic excitations based on TD-DFT. The application to the simulation of CD spectra of oxirane-, chloro-aziridine-, and cyclohexanone derivatives as well as penta- and hexahelicene demonstrates that very good agreement with the results of other TD-DFT implementations is obtained. The agreement with experimental spectra is generally reasonable. Comparison with other computational data shows that it is not very easy to compute the sensitive rotatory strengths accurately. The DFT approach performs quite well here, in particular with the recently developed potentials SAOP and GRAC. Taking the systematic underestimation of excitation energies with the BP86 GGA functional, in particular for Rydberg excitations, for our samples into account, qualitative agreement with experimental spectra can still be achieved with this functional, which allows for assignments and interpretations. However, individual rotatory strengths may change substantially depending on the applied Kohn–Sham potential. Remaining sources of errors, apart from the approximate treatment of DFT itself are, in particular solvent effects, neglect of the effect of molecular vibrations on the spectra, and basis set limitations.

ACKNOWLEDGMENTS

This work has received financial support from the National Science and Engineering Research Council of Canada (NSERC). J.A. thanks Professor Dr. A. Rauk for helpful comments.

[1] E. U. Condon, Rev. Mod. Phys. **9**, 432 (1937).
[2] A. Moscowitz, Adv. Chem. Phys. **4**, 67 (1962).
[3] E. Charney, *The Molecular Basis of Optical Activity* (Wiley, New York, 1979).
[4] A. E. Hansen and T. D. Bouman, Adv. Chem. Phys. **44**, 545 (1980).
[5] *Circular Dichroism: Principles and Applications*, edited by K. Nakanishi, N. Berova, and R. W. Woody (VCH New York, 1994).
[6] E. K. U. Gross and W. Kohn, Adv. Quantum Chem. **21**, 255 (1990).
[7] E. K. U. Gross, J. F. Dobson, and M. Petersilka, Top. Curr. Chem. **181**, 81 (1996).
[8] J. F. Dobson, "Time-dependent density functional theory," in *Electronic Density Functional Theory. Recent Progress and New Directions*, edited

by J. F. Dobson, G. Vignale, and M. P. Das, (Plenum, New York, 1998), pp. 43–53.
[9] R. Bauernschmitt and R. Ahlrichs, Chem. Phys. Lett. **256**, 454 (1996).
[10] J. R. Cheeseman, M. J. Frisch, F. J. Devlin, and P. J. Stephens, J. Phys. Chem. A **104**, 1039 (2000).
[11] P. J. Stephens, F. J. Devlin, J. R. Cheeseman, and M. J. Frisch, J. Phys. Chem. A **105**, 5356 (2001).
[12] F. Furche *et al.*, J. Am. Chem. Soc. **122**, 1717 (2000).
[13] S. Grimme, Chem. Phys. Lett. **339**, 380 (2001).
[14] K. Yabana and G. F. Bertsch, Phys. Rev. A **60**, 1271 (1999).
[15] S. J. A. van Gisbergen, J. G. Snijders, and E. J. Baerends, J. Chem. Phys. **103**, 9347 (1995).
[16] S. J. A. van Gisbergen, J. G. Snijders, and E. J. Baerends, Comput. Phys. Commun. **118**, 119 (1999).
[17] AMSTERDAM DENSITY FUNCTIONAL Program, Theoretical Chemistry, Vrije Universiteit, Amsterdam, http://www.scm.com
[18] G. te Velde and E. J. Baerends, J. Comput. Phys. **99**, 84 (1992).
[19] C. Fonseca Guerra, O. Visser, J. G. Snijders, G. te Velde, and E. J. Baerends, ''Parallelisation of the AMSTERDAM DENSITY FUNCTIONAL program program,'' in *Methods and Techniques for Computational Chemistry*, STEF, Cagliari, 1995.
[20] G. te Velde *et al.*, J. Comput. Chem. **22**, 931 (2001).
[21] C. Jamorski, M. E. Casida, and D. R. Salahub, J. Chem. Phys. **104**, 5134 (1996).
[22] H. H. Heinze, A. Görling, and N. Rösch, J. Chem. Phys. **113**, 2088 (2000).
[23] M. E. Casida, Time-dependent density functional response theory for molecules, in *Recent Advances in Density Functional Methods*, edited by D. P. Chong (World Scientific, Singapore, 1995), Vol. 1.
[24] P. R. T. Schipper, O. V. Gritsenko, S. J. A. van Gisbergen, and E. J. Baerends, J. Chem. Phys. **112**, 1344 (2000).
[25] M. Grüning, O. V. Gritsenko, S. J. A. van Gisbergen, and E. J. Baerends, J. Chem. Phys. **114**, 652 (2001).
[26] A. D. Buckingham, Adv. Chem. Phys. **12**, 107 (1967).
[27] W. Kauzmann, *Quantum Chemistry* (Academic, New York, 1957).
[28] J. Autschbach and T. Ziegler, J. Chem. Phys. **116**, 891 (2002).
[29] F. Furche, J. Chem. Phys. **114**, 5982 (2001).
[30] G. Vignale and M. Rasolt, Phys. Rev. Lett. **59**, 2360 (1987).
[31] G. Vignale and W. Kohn, Phys. Rev. Lett. **77**, 2037 (1996).
[32] G. Vignale, ''Current-density functional theory of linear response to time-dependent electro-magnetic fields,'' in Ref. 8, pp. 199–216.
[33] T. K. Ng, Phys. Rev. Lett. **62**, 2417 (1989).
[34] F. Kootstra, P. L. de Boeij, and J. G. Snijders, J. Chem. Phys. **112**, 6517 (2000).
[35] P. L. de Boeij, F. Kootstra, J. A. Berger, R. van Leeuwen, and J. G. Snijders, J. Chem. Phys. **115**, 1995 (2001).
[36] S. M. Colwell and N. C. Handy, Chem. Phys. Lett. **217**, 271 (1994).
[37] A. M. Lee, N. C. Handy, and S. M. Colwell, J. Chem. Phys. **103**, 10095 (1995).
[38] A. D. McLachlan and M. A. Ball, Rev. Mod. Phys. **36**, 844 (1964).
[39] J. Oddershede, ''Propagator methods,'' in *Ab Initio Methods in Quantum Chemistry*, edited by K. P. Lawley (Wiley, New York, 1987), Vol. II, pp. 201–239.
[40] A. E. Hansen, B. Voigt, and S. Rettrup, Int. J. Quantum Chem. **23**, 595 (1983).
[41] S. J. A. van Gisbergen, C. Fonseca-Guerra, and E. J. Baerends, J. Comput. Chem. **21**, 1511 (2000).
[42] K. D. Bak *et al.*, Theor. Chim. Acta **90**, 441 (1995).
[43] J. Guan *et al.*, J. Chem. Phys. **98**, 4753 (1993).
[44] S. J. A. van Gisbergen *et al.*, Phys. Rev. A **57**, 2556 (1998).
[45] M. E. Casida, C. Jamorski, K. C. Casida, and D. R. Salahub, J. Chem. Phys. **108**, 4439 (1998).
[46] S. H. Vosko, L. Wilk, and M. Nusair, Can. J. Phys. **58**, 1200 (1989).
[47] A. D. Becke, Phys. Rev. A **38**, 3098 (1988).
[48] J. P. Perdew, Phys. Rev. B **33**, 8822 (1986).
[49] J. P. Perdew, Phys. Rev. B **34**, 7406 (1986).
[50] ''Gas phase ion energetics data,'' in *NIST Chemistry WebBook, NIST Standard Reference Database Number 69*, edited by W. G. Mallard and P. J. Linstrom (National Institute of Standards and Technology, Gaithersburg, MD, 2000); data prepared by S. G. Lias, http://webbook.nist.gov
[51] M. Carnell *et al.*, Chem. Phys. Lett. **180**, 477 (1991).
[52] F. Pulm, J. Schramm, J. Hormes, S. Grimme, and S. Peyerimhoff, Chem. Phys. **224**, 143 (1997).
[53] A. Brown, C. M. Kemp, and S. F. Mason, J. Chem. Soc. A **1971**, 751.
[54] W. S. Brickell, A. Brown, C. M. Kemp, and S. F. Mason, J. Chem. Soc. A **1971**, 756.
[55] S. Grimme *et al.*, Chem. Phys. Lett. **213**, 32 (1993).
[56] A. Rauk, J. Am. Chem. Soc. **103**, 1023 (1981).
[57] D. Cohen, M. Levi, H. Basch, and A. Gedanken, J. Am. Chem. Soc. **105**, 1738 (1983).
[58] M. Carnell, S. Grimme, and S. D. Peyerimhoff, Chem. Phys. **179**, 385 (1994).
[59] A. Moscowitz, Tetrahedron **13**, 48 (1961).
[60] J.-H. Pao and D. P. Santry, J. Am. Chem. Soc. **88**, 4157 (1966).
[61] R. R. Gould and R. Hoffmann, J. Am. Chem. Soc. **92**, 1813 (1970).
[62] W. Moffitt, R. B. Woodward, A. Moscowitz, W. Klyne, and C. Djerassi, J. Am. Chem. Soc. **83**, 4013 (1961).
[63] G. V. Shustov, G. K. Kadorkina, R. G. Kostyanovsky, and A. Rauk, J. Am. Chem. Soc. **110**, 1719 (1988).
[64] S. Grimme, J. Harren, A. Sobanski, and F. Vögtle, Eur. J. Org. Chem. **1998**, 1491.
[65] S. Grimme and S. Peyerimhoff, Chem. Phys. **204**, 411 (1996).